JACS
JOURNAL OF THE AMERICAN CHEMICAL SOCIETY

ARTICLE

pubs.acs.org/JACS

Efficient Excited Energy Transfer Reaction in Clay/Porphyrin Complex toward an Artificial Light-Harvesting System

Yohei Ishida,[†,‡] Tetsuya Shimada,[†] Dai Masui,[†] Hiroshi Tachibana,[†] Haruo Inoue,[†] and Shinsuke Takagi*[,†,§]

[†]Department of Applied Chemistry, Graduate Course of Urban Environmental Sciences, Tokyo Metropolitan University, Minami-ohsawa 1-1, Hachiohji, Tokyo 192-0397 Japan

[‡]Japan Society for the Promotion of Science (DC1), Ichibancho, Chiyoda-ku, Tokyo 102-8471, Japan

[§]PRESTO (Precursory Research for Embryonic Science and Technology), Japan Science and Technology Agency, 4-1-8 Honcho Kawaguchi, Saitama, Japan

ABSTRACT: The quantitative excited energy transfer reaction between cationic porphyrins on an anionic clay surface was successfully achieved. The efficiency reached up to ca. 100% owing to the "Size-Matching Rule" as described in the text. It was revealed that the important factors for the efficient energy transfer reaction are (i) suppression of the self-quenching between adjacent dyes, and (ii) suppression of the segregated adsorption structure of two kinds of dyes on the clay surface. By examining many different kinds of porphyrins, we found that tetrakis(1-methylpyridinium-3-yl) porphyrin (*m*-TMPyP) and tetrakis(1-methylpyridinium-4-yl) porphyrin (*p*-TMPyP) are the suitable porphyrins to accomplish a quantitative energy transfer reaction. These findings indicate that the clay/porphyrin complexes are promising and prospective candidates to be used for construction of an efficient artificial light-harvesting system.

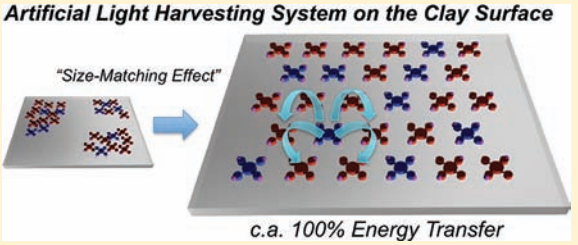

INTRODUCTION

In natural photosynthetic systems such as in purple bacteria, a light-harvesting system (LHS) which is composed of regularly arranged molecules collects the sunlight efficiently and carries the excitation energy smoothly to the reaction center.[1] One of the strategies to realize an efficient artificial LHS is a construction of such regularly arranged structure of functional dyes. A fair amount of research has been carried out to realize an artificial LHS.[2−17] Supramolecular assemblies,[2−11] covalently linked systems[12−15] and dendrimer systems[16,17] have been examined for the same purpose.

Clay minerals[18−24] are an attractive group of materials that are characterized by (1) nanostructured flat sheets, (2) negatively charged surfaces, (3) exfoliation or stack ability of individual nanosheets depending on the surrounding conditions, and (4) optical transparency in the visible region in the exfoliated state, when the particle size is small (ca. <200 nm). We expect that clay minerals can act as ideal host materials to construct structures of dye assemblies for efficient energy transfer reactions. Thus, we have been focusing on using clay minerals as novel host materials for constructing an artificial LHS. We propose the novel nanosheet type LHS in this paper.

Generally, dye molecules tend to aggregate[25] and/or segregate[26] on the clay surface or in the interlayer space between the clay sheets (Figure 1). The aggregation, such as a H-aggregate formation, significantly decreases the excited state lifetimes of dyes. On the other hand, the segregation causes the decrease in reaction efficiency due to decrease of adjacent probabilities of molecules. However, little is known about photochemical reaction processes in clay/dye complexes.[26−29] We have developed a novel technique for the arrangement control of dyes assembly on the clay surface.[30−32] Moreover, we have successfully prepared unique clay/porphyrin complexes in which the porphyrin molecules adsorb on the clay surface without aggregation even at high dye loadings.[30−32] The excited-state lifetime of adsorbed porphyrin is long enough to undergo the photochemical reactions. The formation of these unique hybrids was rationalized by a size-matching of distances between the charged sites in the porphyrin molecule and those between anionic sites on the clay surface. We named this effect as the "Size-Matching Rule".[30−32] We have already studied the excited energy transfer reaction between adsorbed porphyrins on the clay surface.[6−8] In a previous work, the maximum quantum yield for the energy transfer was ∼35% between porphyrins on the clay surface.[6] In our system, the quenching due to an interaction of the transition dipole moments in an aggregation form (Figure 1a) was completely suppressed by the "Size-Matching Rule".[30−32] Thus, the major factors lowering the energy transfer efficiency were supposed to be a self-quenching between porphyrins on the clay surface in a nonaggregated form (Figure 1b), and the segregation structure of two kinds of dyes (Figure 1c). In the present paper, the reaction conditions are optimized in terms of the following aspects: (i) choosing the appropriate porphyrins in which the self-

Received: November 18, 2010
Published: August 02, 2011

dx.doi.org/10.1021/ja204425u | *J. Am. Chem. Soc.* 2011, 133, 14280–14286

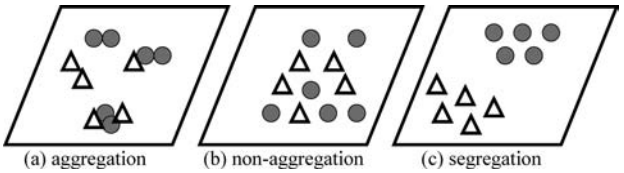

Figure 1. The schematic images of adsorption structures: (a) aggregation, (b) nonaggregation, (c) segregation of two kinds of dyes. In the aggregation structure (a), there is an interaction between transition dipole moments of dyes.

Chart 1. The Structure of Saponite, Having One Octahedral Layer Sandwiched by Two Tetrahedral Layers

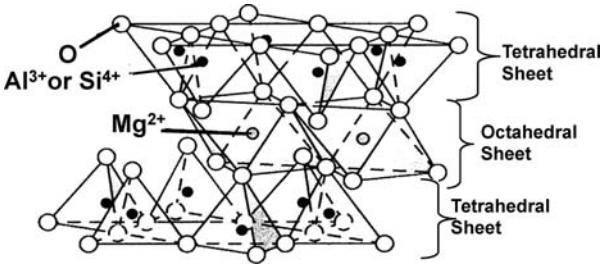

quenching is negligible, (ii) choosing the porphyrins which do not form segregation structure, (iii) adjustment of reaction conditions such as the adsorption density and the donor–acceptor ratio. It should be noted that the energy transfer is significantly affected by the relative configuration of the excited donor and acceptor in terms of κ^2 according to the Förster equation.[33] In a three-dimensional random conformation, the value of κ^2 is 2/3.[34] On the other hand, since the porphyrin dyes adsorb on the two-dimensional clay surface in our system, the value of κ^2 is calculated to be 5/4. Like this, our system is preferred in terms of molecular conformational alignments.

As a result, the quantitative energy transfer between the adsorbed porphyrins on the clay surface was successfully achieved. The mechanism of energy transfer reaction was examined by a time-resolved fluorescence spectroscopy.

EXPERIMENTAL SECTION

Materials. Saponite clay (Chart 1) used in this experiment was synthesized by hydrothermal synthesis.[35] Synthesized clay was analyzed with XRD, XRF, ^{27}Al-NMR, FT-IR, TG, and the intercharge distance on clay surface was calculated to be 1.19 nm on the basis of hexagonal array. Tetrakis(1-methylpyridinium-3-yl) porphyrin (*m*-TMPyP; Chart 2), tetrakis(1-methylpyridinium-2-yl) porphyrin (*o*-TMPyP), zinc tetrakis-(1-methylpyridinium-4-yl) porphyrin (ZnTMPyP), tetrakis(*N*,*N*,*N*-trimethylanilinium-4-yl) porphyrin (H_2TMAP), and zinc tetrakis(*N*,*N*,*N*-trimethylanilinium-4-yl) porphyrin (ZnTMAP) were purchased from Frontier Scientific. Tetrakis(1-methylpyridinium-4-yl) porphyrin (*p*-TMPyP; Chart 2) was purchased from Aldrich. The counterions were exchanged for chloride by use of an ion-exchange column (Organo Amberlite IRA400JCL). The purity of porphyrins was checked by ^{1}H NMR. Water was deionized with an ORGANO BB-5A system (PF filter ×2 + G-10 column).

Analysis. Absorption spectra were measured with Shimadzu UV-3150 spectrophotometer. The corrected fluorescence spectra were measured with Jasco FP-6500 spectrofluorometer. In absorption and fluorescence measurements, a quartz cell was used for the aqueous clay/porphyrin solutions. TG/DTA measurement was carried out with Shimadzu DTG-60H to determine the water contents of porphyrins and clay. The time-resolved fluorescence measurement was conducted under a photon-counting condition (Hamamatsu Photonics, C4334 streak scope, connected with CHROMEX 250IS polychrometer) with EKSPLA PG-432 optical parametric generator (430 nm, 25-ps fwhm, 20 μJ, 1 kHz) pumped by the third harmonic radiation of Nd^{3+}-YAG laser, EKSPLA PL2210JE (355 nm, 25-ps fwhm, 300 μJ, 1 kHz). The laser flux was reduced with neutral density filters to avoid multiphoton absorption processes and nonlinear effects. The time-resolved fluorescence spectra were not corrected; thus, the obtained spectral shape was not the same as the steady-state fluorescence spectroscopy even for the same condition.

Chart 2. The Structures of Tetrakis(1-methylpyridinium-3-yl) Porphyrin (*m*-TMPyP) and Tetrakis(1-methylpyridinium-4-yl) Porphyrin (*p*-TMPyP)[a]

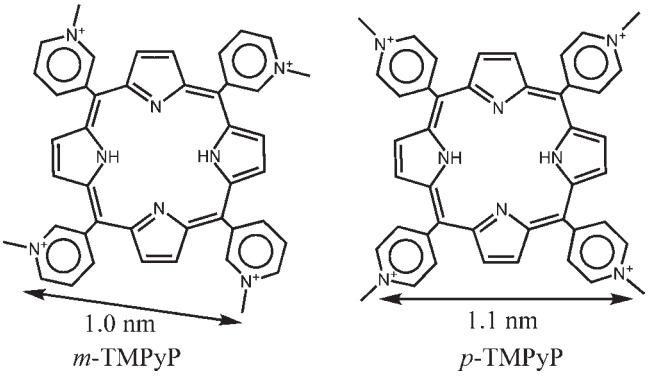

[a]The distances between cationic parts in the pophyrins are indicated.

Preparation Methods for the Clay/Porphyrin Complexes. Typical procedure for preparation of the clay/porphyrin complexes was as follows. In this experiment, *m*-TMPyP(D) and *p*-TMPyP(A) were used as an energy donor and an energy acceptor, respectively. Aqueous solutions of *m*-TMPyP(D) and *p*-TMPyP(A) were mixed. The obtained solutions were mixed with an aqueous clay solution (9.9 mg L^{-1}) under vigorous stirring. The total concentrations of *m*-TMPyP(D) and *p*-TMPyP(A) were 1.0×10^{-7} M. The molar ratio of *m*-TMPyP(D) to *p*-TMPyP(A) was modulated as *m*-TMPyP(D)/*p*-TMPyP(A) = 15/1, 8/1, 3/1, 1/1, 1/3, 1/8, 1/15. The porphyrin loading level versus cation exchange capacity (CEC) of the clay was adjusted from 0.05 to 90% by changing the volume of the clay solution. Under these conditions, the clay sheets exist in a form of individually exfoliated sheets and the obtained solution was substantially transparent. Since no porphyrin was detected in supernatant liquid obtained by a centrifugation of clay/porphyrin mixture (12 000 rpm, 60 min), all porphyrin molecules adsorb on the clay surface.

RESULTS AND DISCUSSION

The Self-Quenching Behavior of the Tetra-Cationic Porphyrins on the Clay Surface. The self-quenching behavior of the porphyrins on the clay surface was examined by measuring the fluorescence spectra. We selected the six porphyrins in terms of the difference of the intracharge distance in the molecule and the adsorption strength onto the clay surface. The self-quenching is induced by the electron transfer from an excited porphyrin to the adjacent identical porphyrin at ground state in the present system. The self-quenching decreases the excited singlet lifetime of dyes, and thus, decreases the energy transfer efficiency.[8,36]

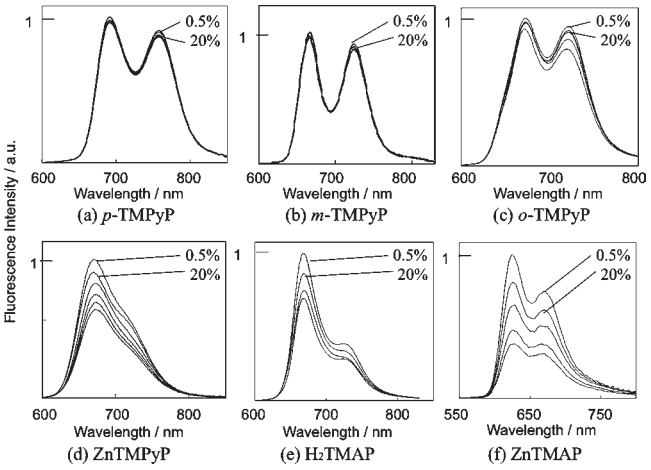

Figure 2. The fluorescence spectra of porphyrins on the clay surface when the loading levels of porphyrin were set at 0.5, 20, 40, 60, 80% vs CEC of the clay. (a) *p*-TMPyP, (b) *m*-TMPyP, (c) *o*-TMPyP, (d) ZnTMPyP, (e) H_2TMAP, (f) ZnTMAP. [porphyrin] = 1.0×10^{-7} M. The excitation wavelengths were set at λ_{max} of each porphyrin, (a) 450 nm, (b) 430 nm, (c) 421 nm, (d) 460 nm, (e) 424 nm, (f) 429 nm.

To construct the efficient energy transfer systems, reducing the self-quenching behavior is essential. In the present work, the self-quenching behavior was quantitatively discussed by determining the self-quenching ratio. The self-quenching ratio was defined as $(I_f^0 - I_f)/I_f^0$, where I_f is the fluorescence intensity of porphyrin when the loading level is 20% versus CEC of the clay, and I_f^0 is that at 0.5% versus CEC of the clay. At 0.5% adsorption, the self-quenching was negligible; thus, it can be used as the standard fluorescence intensity. Under the present experimental condition, the concentration of porphyrin dyes is always kept constant to be 1.0×10^{-7} M and the loading level of adsorption is varied by controlling the concentration of clay, indicating that every sample adsorbed the same number of photons under the same absorbance. We can thus discuss the self-quenching, $(I_f^0 - I_f)/I_f^0$, by simply comparing the fluorescence intensity. The observed fluorescence spectra of each porphyrin, when their loading was changed from 0.5% to 80% versus CEC, are shown in Figure 2.

As reported before, the self-quenching of the excited state of *p*-TMPyP was not observed on the clay surface even at a high density adsorption condition (Figure 2a).[36] In the case of *o*-TMPyP, ZnTMPyP, H_2TMAP, and ZnTMAP on the clay surface, the moderate self-quenching was observed (Figure 2c–f). The self-quenching ratios were 4, 12, 14, and 21%, respectively, when their loading levels were 20% versus CEC of the clay. It should be noted that the self-quenching of these porphyrins is still less than that of typical dyes. This is due to the effect of the "Size-Matching Rule" which fixes the dyes with an appropriate intermolecular distance. Among examined porphyrins, the self-quenching of *m*-TMPyP on the clay surface was found to be almost negligible (0.2% quenching at 20% CEC, as shown in Figure 2b) similarly to *p*-TMPyP. Thus, these two porphyrins were selected to examine the energy transfer reactions. It is assumed that one of the factors to determine the self-quenching efficiency is the adsorption strength of the porphyrin molecules onto the clay surface. The details will be published in the near future.

The Absorption and Fluorescence Spectra of Clay/Porphyrin Complexes. The absorption and fluorescence spectra of

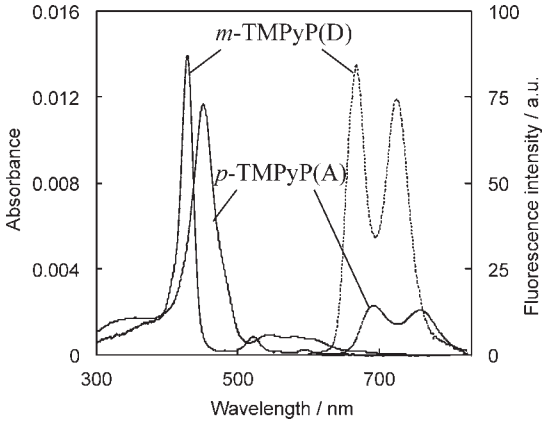

Figure 3. The absorption (solid line) and fluorescence (dashed line, λ_{ex} = 430 nm) spectra of *m*-TMPyP(D)/clay and *p*-TMPyP(A)/clay complexes in the aqueous suspension ([clay] = 9.9 mg L^{-1}, [*m*-TMPyP(D)] = [*p*-TMPyP(A)] = 5.0×10^{-8} M).

m-TMPyP(D)/clay and *p*-TMPyP(A)/clay complexes were relatively well differentiated (Figure 3). The absorption spectra of *m*-TMPyP(D)/*p*-TMPyP(A)/clay complexes were completely identical with a sum of individual absorption spectra of *m*-TMPyP(D)/clay and *p*-TMPyP(A)/clay complexes. Thus, it was found that porphyrin aggregation is completely suppressed and the porphyrin exists as a single molecule for a whole loading range (0.05–90% vs CEC of the clay) even when two porphyrins coexist on the clay surface. The fluorescence intensity is governed by the absorbance at excitation wavelength (430 nm) and its fluorescence quantum yield. The extinction coefficients of *m*-TMPyP(D) and *p*-TMPyP(A) at 430 nm are 280 000 and 114 000 M^{-1} cm^{-1}, respectively, and the fluorescence quantum yields are 0.081 and 0.048, respectively.

The spectral overlap between the fluorescence spectrum of donor and the absorption of acceptor is an important factor for determining the energy transfer rate constant, according to eq 1.[33]

$$k_{ET} = \frac{9000 \ln 10 \kappa^2 \phi}{128 \pi^5 n^4 N \tau_{Donor} R^6} J \quad (1)$$

where κ is the orientation parameter (κ^2 = 5/4 for in-plane orientation[34]), φ is the fluorescence quantum yield of donor, n is the refractive index of the bulk medium (n = 1.33 in the case of water), N is the Avogadro constant, τ_{Donor} is the excited singlet lifetime of donor on the clay surface, and R is the center-to-center distance between adsorbed porphyrins.

According to the analysis of the overlap between the fluorescence of *m*-TMPyP(D) and the absorption of *p*-TMPyP(A), based on eq 2,[37] the overlap integral (J) is calculated to be 3.9×10^{-14} M^{-1} cm^{-1} nm^4.

$$J = \sum F_d(\lambda) \varepsilon_a(\lambda) \lambda^4 \Delta\lambda \quad (2)$$

where λ is the wavelength (in cm), ε_a (λ) is the extinction coefficient of the acceptor at wavelength λ and F_d (λ) is the fraction of the total fluorescence intensity of the donor. This obtained value is not large compared to typical energy transfer systems,[37] but would be large enough if other factors for energy transfer are suitable.

The Energy Transfer Reaction from *m*-TMPyP to *p*-TMPyP on the Clay Surface. *m*-TMPyP(D) was used as

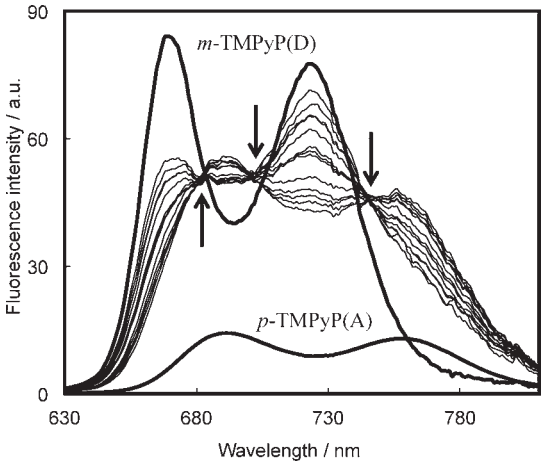

Figure 4. The fluorescence spectra for *m*-TMPyP(D)/*p*-TMPyP(A)/clay complexes excited at 430 nm in aqueous solution. [*m*-TMPyP(D)] = [*p*-TMPyP(A)] = 5.0×10^{-8} M. The porphyrin loading levels were set at 0.05−90% vs CEC of the clay. The thick lines are individual fluorescence spectra of *m*-TMPyP(D)/clay and *p*-TMPyP(A)/clay complexes. The arrows indicate isoemissive points.

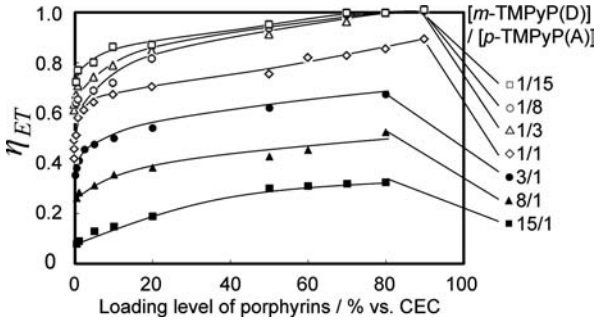

Figure 5. The energy transfer efficiencies at various loading levels and ratios of porphyrins. [*m*-TMPyP(D)] + [*p*-TMPyP(A)] = 1.0×10^{-7} M, [*m*-TMPyP(D)]/[*p*-TMPyP(A)] = 15/1 (■), 8/1 (▲), 3/1 (●), 1/1 (◇), 1/3 (△), 1/8 (○), 1/15 (□). The porphyrin loading levels were set at 0.05−90% vs CEC of the clay in aqueous solution.

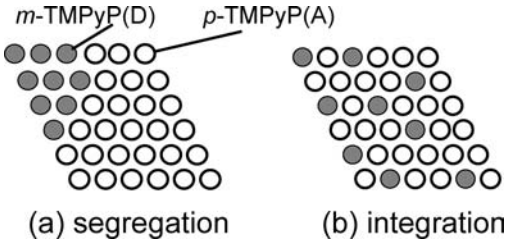

Figure 6. Possible ideal images of segregation (a) and integration (b) adsorption structure of two kinds of porphyrins on the clay surface in the case of *m*-TMPyP(D)/*p*-TMPyP(A) = 1/3.

an energy donor, and *p*-TMPyP(A) was used as an energy acceptor. The energy transfer from the excited singlet state of *m*-TMPyP(D) to the ground state of *p*-TMPyP(A) on the clay surface was examined at various loading levels of porphyrins (0.05−90% vs CEC). The excitation wavelength was set at 430 nm, which is the λ_{max} of *m*-TMPyP(D)/clay complex, for all experiments. *m*-TMPyP(D) absorbed the 71% of the excitation light under the ratio of *m*-TMPyP/*p*-TMPyP = 1/1. The absorption spectra exhibited a completely identical shape at all loading levels of porphyrins. The fluorescence spectral change at various loading levels of porphyrin when *m*-TMPyP(D)/*p*-TMPyP(A) was set at 1/1, is shown in Figure 4. The clear isoemissive points were observed as indicated by the arrows in Figure 4.

Since the absorption and fluorescence spectra are relatively differentiated, the energy transfer efficiency can be quantitatively estimated by the analysis of fluorescence spectra.[8] The fluorescence spectra of *m*-TMPyP(D)/*p*-TMPyP(A)/clay complexes can be well simulated as a superposition of the respective fluorescence spectra of *m*-TMPyP(D)/clay and *p*-TMPyP(A)/clay complexes. The calculation procedure of the energy transfer efficiency (η_{ET}) and the self-quenching efficiency (ϕ_q) is as follows.

The total fluorescence of *m*-TMPyP(D)/*p*-TMPyP(A)/clay complex ($F_{ET}(\nu)$) can be expressed by eq 3.

$$F_{ET}(\nu) = (1 - \eta_{ET} - \phi_q) \times F_m^0(\nu) + \left(1 + \frac{1 - 10^{-A_m}}{1 - 10^{-A_p}}\eta_{ET}\right) \times F_p^0(\nu) \quad (3)$$

where $F_{ET}(\nu)$ is the fluorescence spectrum of *m*-TMPyP(D)/*p*-TMPyP(A)/clay complex, $F_m{}^0(\nu)$ is the fluorescence spectrum of *m*-TMPyP(D)/clay complex, $F_p{}^0(\nu)$ is the fluorescence spectrum of *p*-TMPyP(A)/clay complex, η_{ET} is the energy transfer efficiency, defined in eq 4, ϕ_q is the quenching efficiency due to the electron transfer between same porphyrins or two kinds of porphyrins, defined in eq 5, A_m is the absorbance of *m*-TMPyP(D)/clay complex at 430 nm, and A_p is the absorbance of *p*-TMPyP(A)/clay complex at 430 nm.

$$\eta_{ET} = \frac{k_{ET}}{k_{ET} + k_d^m + k_f^m + k_q} \quad (4)$$

$$\phi_q = \frac{k_q}{k_{ET} + k_d^m + k_f^m + k_q} \quad (5)$$

where $k_d{}^m$ is the sum of the nonradiative deactivation rate constant and intersystem crossing rate constant of *m*-TMPyP(D), $k_f{}^m$ is the radiative deactivation rate constant of *m*-TMPyP(D), k_q is the electron transfer rate constant from the excited state of *m*-TMPyP(D) to the ground state of *m*-TMPyP(D) or *p*-TMPyP(A) and k_{ET} is the energy transfer rate constant. Self-quenching of donor porphyrin is induced by this electron transfer (k_q) in the present system.

Under the condition of the ratio of *m*-TMPyP(D)/*p*-TMPyP(A) = 1/1, $A_m = 1.4 \times 10^{-2}$ and $A_p = 5.7 \times 10^{-3}$. On the basis of eq 3, the fluorescence spectrum, $F_{ET}(\nu)$, was simulated with the use of the respective reference fluorescence spectra, $F_m{}^0(\nu)$ and $F_p{}^0(\nu)$. Thus, parameters η_{ET} and ϕ_q can be obtained from the spectral simulation.

In Figure 5, the obtained values of η_{ET} are plotted versus the loading levels of porphyrins. Amazingly, the maximum energy transfer efficiency was ca. 100% (the error range is 100 ± 5%), when *m*-TMPyP(D)/*p*-TMPyP(A) = 1/3, 1/8, 1/15 and the loading level of porphyrin was 90% versus CEC. The energy transfer efficiency increased as the loading level of porphyrin increased, since the average intermolecular distances between porphyrins decreased. The Förster type energy transfer rate

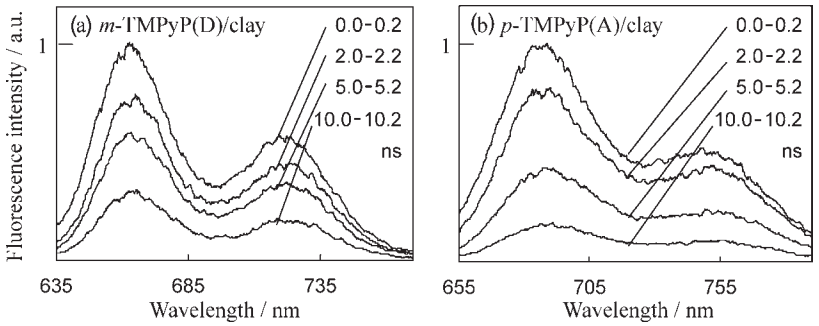

Figure 7. The time-resolved fluorescence spectra for (a) *m*-TMPyP(D)/clay and (b) *p*-TMPyP(A)/clay complexes at 0.0−0.2, 2.0−2.2, 5.0−5.2, and 10.0−10.2 ns after excitation. The excitation wavelength was 430 nm. The dye loadings were set at 20% vs CEC of the clay. [*m*-TMPyP(D)] = [*p*-TMPyP(A)] = 1.0×10^{-7} M.

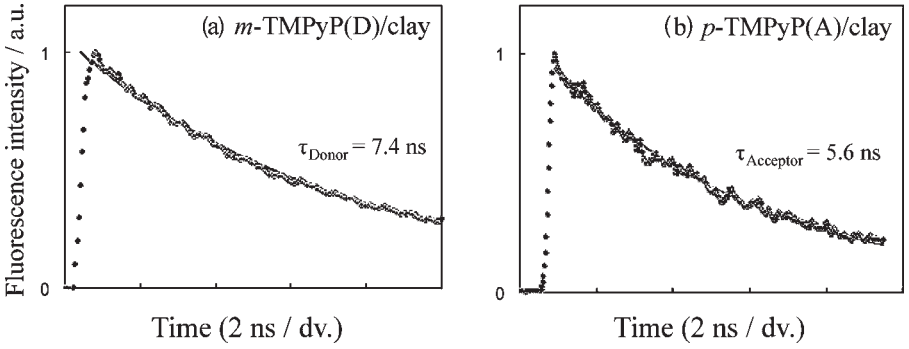

Figure 8. The fluorescence decay profiles of (a) *m*-TMPyP(D)/clay and (b) *p*-TMPyP(A)/clay complexes. The obtained values (●) and the fitted curves (solid line) are shown. The excitation wavelength was 430 nm. The dyes loadings were set at 20% vs CEC of the clay. [*m*-TMPyP(D)] = [*p*-TMPyP(A)] = 1.0×10^{-7} M.

constant is inversely proportional to the sixth power of the intermolecular distance.[33] The energy transfer efficiency increased by increasing the ratio of *p*-TMPyP on the clay surface, because the number of energy acceptor (*p*-TMPyP) around the donor porphyrin molecules (*m*-TMPyP) significantly affected the energy transfer rate.

Under all experimental conditions, ϕ_q values were always zero. This indicates that the quenching process due to the electron transfer between porphyrins did not occur on the clay surface. It was revealed that selecting the porphyrins in which self-quenching is negligible on the clay surface was an important factor to decrease the electron transfer rate and to achieve the quantitative energy transfer.

In the case of *m*-TMPyP(D)/*p*-TMPyP(A) = 1/3, 1/8, 1/15, the efficiencies of energy transfer at high loading levels (80 and 90% vs CEC of the clay) were same (∼100%). From these results, the adsorption structure of two porphyrins on the clay surface can be discussed. Generally, two kinds of dyes segregate each other when the dyes co-adsorb on the clay surface.[26] If two kinds of porphyrins had co-adsorbed on the clay surface with segregation (Figure 6a), the energy transfer efficiencies would not have reached up to 100%, because the donor porphyrins which are surrounded by donor porphyrins themselves could not transfer the excited energy to the acceptor porphyrin. Therefore, an ideal arrangement of two kinds of co-adsorbed porphyrins on the clay surface could be depicted in Figure 6b, as a typical one of the possible arrangements, where each donor molecule is surely surrounded by acceptor molecules. In the clay−porphyrin complexes, there is little interaction between adsorbed porphyrins due to the effect of the "Size-Matching Rule". Thus, integration (Figure 6b) was realized in the present complexes.

The Time-Resolved Fluorescence Measurements for Clay/Porphyrin Complexes. The time-resolved fluorescence spectra for clay/porphyrin complexes were measured using the picoseconds fluorescence measurement system. At first, the time-resolved fluorescence measurements for *m*-TMPyP(D)/clay and *p*-TMPyP(A)/clay complexes were examined. In this experiment, the concentrations of porphyrins were set at 20% loadings versus CEC of the clay ([*m*-TMPyP(D)] = [*p*-TMPyP(A)] = 1.0×10^{-7} M) and the samples were excited at 430 nm. The obtained time-resolved fluorescence spectra and the decay curves are shown in Figures 7 and 8, respectively. As shown in Figure 7, the fluorescence spectral shapes of *m*-TMPyP(D)/clay and *p*-TMPyP(A)/clay complexes were completely the same during the decay. As shown in Figure 8, the decay curves of *m*-TMPyP(D)/clay and *p*-TMPyP(A)/clay complexes can be analyzed as a single exponential decay. The excited single lifetimes of *m*-TMPyP(D)/clay and *p*-TMPyP(A)/clay complexes are calculated to be 7.4 ± 0.1 ns (τ_{Donor}) and 5.6 ± 0.1 ns ($\tau_{Acceptor}$), respectively. The photochemical behavior of dyes on the inorganic surface tends to be complicated due to the aggregate formation and self-quenching behavior. It should be noted that simple decay curves were observed in the present system. In addition, it is interesting that the obtained $\tau_{Acceptor}$ (5.6 ns) is longer than that in an aqueous solution without clay (5.1 ns). Like this, the dye that fulfills the "Size-Matching Rule" exhibits very unique photochemical properties on the clay surface.

dx.doi.org/10.1021/ja204425u |*J. Am. Chem. Soc.* 2011, 133, 14280–14286

The time-resolved fluorescence spectra for *m*-TMPyP(D)/*p*-TMPyP(A)/ complexes were examined to elucidate the details of energy transfer reaction. In the experiment, the ratio of donor/acceptor porphyrin was *m*-TMPyP(D)/*p*-TMPyP(A) = 1/3, and the total concentration of porphyrins was set at 90% loadings versus CEC of the clay. In such conditions, the η_{ET} value determined with steady-state fluorescence experiment was ca. 100% as shown in Figure 5. The observed time-resolved fluorescence spectra for *m*-TMPyP(D)/*p*-TMPyP(A)/clay complex excited at 430 nm were shown in Figure 9. The change of spectral shape obviously indicates the energy transfer from excited donor porphyrin to acceptor porphyrin. At 4.0−4.2 ns, the obtained spectrum agreed well with that of *p*-TMPyP(A)/clay.

The fluorescence decay analysis for *m*-TMPyP(D)/*p*-TMPyP-(A)/clay complex was conducted in order to estimate the energy transfer rate constant (k_{ET}). In Figure 10, the fluorescence decay curves for *m*-TMPyP(D)/*p*-TMPyP(A)/clay complex in the region of (a) 635−655 nm and (b) 770−790 nm are shown. The region of 635−655 nm mainly corresponds to the fluorescence region of *m*-TMPyP(D), and the region of 770−790 nm almost corresponds to the fluorescence region of *p*-TMPyP(A). As shown in Figure 10a, the decay curve of *m*-TMPyP(D)/*p*-TMPyP(A)/clay at 635−655 nm can be analyzed as double exponentials decay. The lifetimes are calculated to be 0.4 ± 0.1 ns (τ_1) and 5.6 ± 0.1 ns (τ_2), respectively. τ_2 agrees well with $\tau_{Acceptor}$ and the decay curve does not consist of the component with τ_{Donor} (7.4 ns). These results suggest that the short lifetime component (τ_1) is derived from the excited energy transfer from *m*-TMPyP(D) to the adjacent *p*-TMPyP(A) on the clay surface.

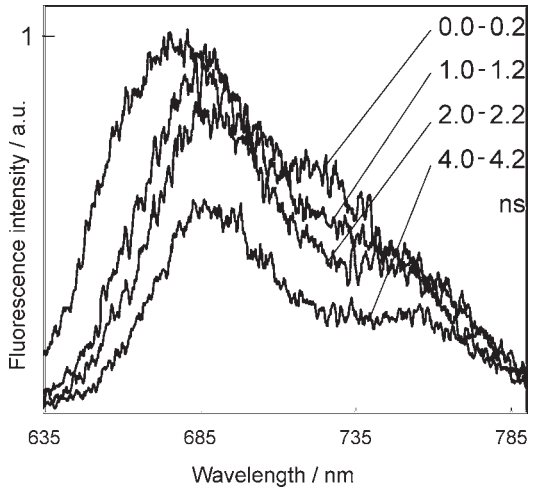

Figure 9. The time-resolved fluorescence spectra for *m*-TMPyP(D)/*p*-TMPyP(A)/clay complex at 0.0−0.2, 1.0−1.2, 2.0−2.2, and 4.0−4.2 ns after excitation. The excitation wavelength was 430 nm. The sum of dyes loadings was set at 90% vs CEC of the clay. *m*-TMPyP(D)/*p*-TMPyP(A) = 1/3 and [*m*-TMPyP(D)] + [*p*-TMPyP(A)] = 1.0×10^{-7} M.

In case of the decay curve of *m*-TMPyP(D)/*p*-TMPyP(A)/clay complex at 770−790 nm (Figure 10b), the rise and decay components which can be analyzed as double exponentials were obviously observed. The lifetimes are calculated to be 0.4 ± 0.1 ns (τ_3) and 5.6 ± 0.1 ns (τ_4) for the rise and decay components, respectively. The obtained lifetime value of rise component (τ_3) in the region of 770−790 nm completely agrees with that of decay component (τ_1) in the region of 635−655 nm. Thus, it can be concluded that τ_1 and τ_3 are the component derived from the energy transfer reaction.

From the values of the short lifetime (τ_1 or τ_3 = 0.4 ± 0.1 ns) and lifetime of donor porphyrin (τ_{Donor} = 7.4 ± 0.1 ns), the energy transfer rate constant k_{ET} can be obtained with eq 6. The obtained value of k_{ET} is 2.4 ± 0.6 × 10^9 s^{-1}.

$$k_{ET} = 1/\tau_1 - 1/\tau_{Donor} = 1/\tau_3 - 1/\tau_{Donor} \quad (6)$$

where τ_1 and τ_3 (= $1/(k_{ET} + k_d^m + k_f^m)$) is the short lifetime of *m*-TMPyP(D)/ *p*-TMPyP(A)/clay complex in the presence of *p*-TMPyP(A), τ_{Donor} (= $1/(k_d^m + k_f^m)$) is the lifetime of m-TMPyP(D) /clay complex in the absence of *p*-TMPyP(A).

The energy transfer efficiency (η_{ET}') calculated by the values of k_{ET} and τ_{Donor} is 95 ± 1% according to eq 7. This value agrees well with the observed value with steady-state fluorescence experiment, 99.7 ± 5% (Figure 5).

$$\eta_{ET}' = \frac{k_{ET}}{k_{ET} + k_d^m + k_f^m} = \frac{k_{ET}}{k_{ET} + \tau_{Donor}^{-1}} \quad (7)$$

From these results, the Förster distance (R_0),[33] which is the distance between fluorophores at which the energy transfer rate is equal to the fluorescence decay rate, is calculated to be 4.2 ± 0.2 nm according to eq 8[33] based on the Förster mechanism,

$$k_{ET} = \frac{1}{\tau_{Donor}}\left(\frac{R_0}{R}\right)^6 \quad (8)$$

where R is the center-to-center distance between adsorbed porphyrins. In the present system, R is calculated to be 2.6 nm when the dye loading was 90% versus CEC of the clay on the

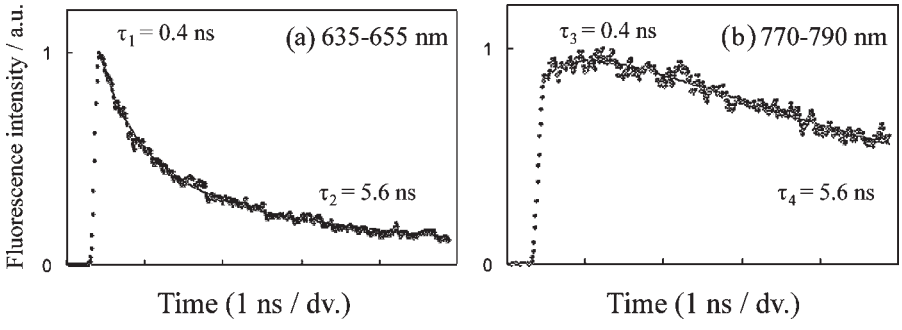

Figure 10. The fluorescence decay profiles of *m*-TMPyP(D)/ *p*-TMPyP(A)/clay complex in the region of (a) 635−655 nm and (b) 770−790 nm. The region of 635−655 nm mainly corresponds to the fluorescence of *m*-TMPyP(D)/clay, and the region of 770−790 nm almost corresponds to the fluorescence of *p*-TMPyP(A)/clay. The obtained values (●) and the fitted curves (solid line) are shown. The conditions of samples were 90% dyes loadings vs CEC of the clay, *m*-TMPyP(D)/*p*-TMPyP(D) = 1/3 and [*m*-TMPyP(D)] + [*p*-TMPyP(A)] = 1.0×10^{-7} M.

dx.doi.org/10.1021/ja204425u |*J. Am. Chem. Soc.* 2011, 133, 14280–14286

basis of hexagonal allay. It should be noted that donor porphyrin was surrounded by 4.5 acceptor porphyrins in the ideal condition.

Interestingly, the obtained value of R_0 is rather large in spite of the small J value. One of the major factors for the large R_0 value is the orientation parameter κ^2 (eq 1). The value of κ^2 is 2/3 for a randomly oriented molecule in three-dimensional system. In the present system, since porphyrin molecules adsorb on the two-dimensional clay surface, κ^2 is calculated to be 5/4.[34] Like this, the energy transfer on the clay surface is preferred in terms of κ^2.

It is also interesting that k_{ET} could be analyzed as only one component. This strongly indicates that porphyrin molecules do not aggregate and the intermolecular distance is uniform on the clay surface. In usual photochemical reactions on solid surfaces, the photochemical behavior of dyes is complicated due to the variety of intermolecular distances. In our system, porphyrin molecules are strongly adsorbed on the clay surface by the effect of "Size-Matching Rule"; thus, they have appropriate uniform intermolecular distances.

CONCLUSION

In the present paper, the quantitative excited singlet energy transfer reaction between adsorbed porphyrins on the clay surface was successfully achieved. The major factors for the quantitative energy transfer reaction were (i) suppression of the self-quenching due to the excited electron transfer, and (ii) realizing the integrated adsorption structure of two kinds of dyes on the clay surface. The time-resolved fluorescence measurements also indicated that the factors were realized. These factors were controlled by the effect of "Size-Matching Rule". According to this idea, it is presumed that this efficient energy transfer system can be extended to the wide range of dye, which fulfills "Size-Matching Rule". Generally, almost 100% energy transfer efficiency is a crucial requirement to construct artificial LHSs involving multiple-step energy transfers processes. Judging from the results, clay/porphyrin complexes are very promising candidates for photochemical reactions such as an efficient artificial LHS.

AUTHOR INFORMATION

Corresponding Author
takagi-shinsuke@tmu.ac.jp

ACKNOWLEDGMENT

This work has been partly supported by a Grant-in-Aid for Precursory Research for Embryonic Science and Technology (PRESTO) from Japan Science and Technology Agency (JST), and JSPS Research Fellow DC1 from Japan Society for the Promotion of Science.

REFERENCES

(1) Mcdermott, G.; Prince, S. M.; Freer, A. A.; Hawthornthwaite-Lawless, A. M.; Papiz, M. Z.; Cogdell, R. J.; Isaacs, N. W. *Nature* **1995**, *374*, 517–521.
(2) Inagaki, S.; Ohtani, O.; Goto, Y.; Okamoto, K.; Ikai, M.; Yamanaka, K.; Tani, T.; Okada, T. *Angew. Chem., Ind. Ed.* **2009**, *48*, 4042–4046.
(3) Miyatake, T.; Tamiaki, H.; Holzwarth, A. R.; Schaffner, K. *Photochem. Photobiol.* **1999**, *69*, 448–456.
(4) Casey, J. P.; Bachilo, S. M.; Weisman, R. B. *J. Mater. Chem.* **2008**, *18*, 1510–1516.
(5) Kaschak, D. M.; Lean, J. T.; Waraksa, C. C.; Saupe, G. B.; Usami, H.; Mallouk, T. E. *J. Am. Chem. Soc.* **1999**, *121*, 3435–3445.
(6) Takagi, S.; Tryk, D. A.; Inoue, H. *J. Phys. Chem. B* **2002**, *106*, 5455–5460.
(7) Takagi, S.; Eguchi, M.; Tryk, D. A.; Inoue, H. *Langmuir* **2006**, *22*, 1406–1408.
(8) Takagi, S.; Eguchi, M.; Inoue, H. *Res. Chem. Intermed.* **2007**, *33*, 177–189.
(9) Takahashi, R.; Kobuke, Y. *J. Am. Chem. Soc.* **2003**, *125*, 2372–2373.
(10) Fujii, K.; Iyi, N.; Hashizume, H.; Shimomura, S.; Ando, T. *Chem. Mater.* **2009**, *21*, 1179–1181.
(11) Kuroda, T.; Fujii, K.; Sakoda, K. *J. Phys. Chem. C* **2010**, *114*, 983–989.
(12) Schanze, K.; Silverman, E. E.; Zhao, X. *J. Phys. Chem. B* **2005**, *109*, 18451–18459.
(13) Kelley, R. F.; Lee, S. J.; Wilson, T. M.; Nakamura, Y.; Tiede, D. M.; Osuka, A.; Hupp, J. T.; Wasielewski, M. R. *J. Am. Chem. Soc.* **2008**, *130*, 4277–4284.
(14) Yoo, H.; Yang, J.; Nakamura, Y.; Aratani, N.; Osuka, A.; Kim, D. *J. Am. Chem. Soc.* **2009**, *131*, 1488–1494.
(15) Miller, M. A.; Lammi, R. K.; Prathapan, S.; Holten, D.; Lindsey, J. S. *J. Org. Chem.* **2000**, *65*, 6634–6649.
(16) Gilat, S. L.; Adronov, A.; Frechet, Jean, M. J. *Angew. Chem., Int. Ed.* **1999**, *38*, 1422–1427.
(17) Choi, H. -S.; Aida, T.; Yamazaki, T.; Yamazaki, I. *Chem.—Eur. J.* **2002**, *8*, 2667–2678.
(18) Ogawa, M.; Kuroda, K. *Chem. Rev.* **1995**, *95*, 399–438.
(19) Takagi, K.; Shichi, T. *J. Photochem. Photobiol., C* **2000**, *1*, 113–130.
(20) Takagi, S.; Eguchi, M; Tryk, D, A.; Inoue, H. *J. Photochem. Photobiol., C* **2006**, *7*, 104–126.
(21) Thomas, J. K. *Chem. Rev.* **1993**, *93*, 301–320.
(22) Bujdak, J.; Komadel, P. *J. Phys. Chem. B* **1997**, *101*, 9065–9068.
(23) Ras, R.; Umemura, Y.; Johnston, C.; Yamagishi, A.; Schoonheydt, R. *Phys. Chem. Chem. Phys.* **2007**, *9*, 918.
(24) Lopez Arbeloa, F.; Martinez Martıınez, V.; Arbeloa, T.; Lopez Arbeloa, I. *J. Photochem. Photobiol., C* **2007**, *8*, 85.
(25) Bujdak, J.; Iyi, N.; Fujita, T. *Clay Minerals* **2002**, *37*, 121–133.
(26) Pushpito, G. K.; Bard, A. *J. Phys. Chem.* **1984**, *88*, 5519–5526.
(27) Viaene, K.; Caigui, J.; Schoonheydt, R. A.; De Schryver, F C. *Langmuir* **1987**, *3*, 107–111.
(28) Madhavan, D.; Pitchumani, K. *Tetrahedron* **2002**, *58*, 9041–9044.
(29) Menager, M.; Siampiringue, M.; Sarakha, M. *J. Photochem. Photobiol., A* **2009**, *208*, 159–163.
(30) Takagi, S.; Shimada, T.; Yui, T.; Inoue, H. *Chem. Lett.* **2001**, *30*, 128–129.
(31) Takagi, S.; Shimada, T.; Eguchi, M.; Yui, T.; Yoshida, H.; Tryk, D. A.; Inoue, H. *Langmuir* **2002**, *18*, 2265–2272.
(32) Eguchi, M.; Takagi, S.; Tachibana, H.; Inoue, H. *J. Phys. Chem. Solids* **2004**, *65*, 403–407.
(33) Förster, Th. Z. *Discuss. Faraday Soc.* **1959**, *27*, 7–17.
(34) Baumann, J.; Fayer, D., M. *J. Chem. Phys.* **1986**, *85*, 4087–4107.
(35) Egawa, T.; Watanabe, H.; Fujimura, T.; Ishida, Y.; Yamato, M.; Masui, D.; Shimada, T.; Tachibana, H.; Yoshida, H.; Inoue, H.; Takagi, S. *Langmuir* **2011**in press.
(36) Takagi, S.; Eguchi, M.; Yui, T.; Inoue, H. *Clay Sci.* **2006**, *12* (Suppl. 2), 82–87.
(37) Brown, S. R.; Brennan, D. J.; Krull, J. U. *J. Chem. Phys.* **1994**, *100*, 6019–6027.